Int. J. Heat Mass Transfer. Vol. 35, No. 12, pp. 3479–3484, 1992
Printed in Great Britain

0017-9310/92 \$5.00+0.00

TECHNICAL NOTES

Visible and infra-red sensitivity of Rayleigh limit and Penndorf extension to complex refractive index of soot

AHMET SELAMET
Department of Mechanical Engineering and Applied Mechanics,
The University of Michigan, Ann Arbor, MI 48109, U.S.A.

(*Received* 1 *April* 1991 *and in final form* 26 *September* 1991)

1. INTRODUCTION

THE RAYLEIGH limit of the classical Lorenz–Mie (LM) theory is widely utilized in thermal radiation when the particle diameter is small relative to the wavelength of radiation [1–4]. This approximation is usually assumed to be accurate up to the size parameter $\alpha = \pi D/\lambda \cong 0.3$, D being the particle diameter, λ the wavelength of radiation. The extension of Rayleigh bound from $\alpha \cong 0.3$ to $\alpha \cong 0.8$ has been suggested by Penndorf [5] and employed by Ku and Felske [6], and Selamet and Arpaci [7, 8]. Selamet and Arpaci have also assessed the upper bounds of the two approximations by examining the percent error involved in the range $1.5 \leqslant n \leqslant 2.5$ and $0.5 \leqslant k \leqslant 1.5$, n and k being respectively refractive and absorptive index of particles, and applied the Penndorf expansion to soot and thermal radiation interaction.

The present study makes an improved assessment of the foregoing optical property range for soot by employing the Lorentz dispersion theory [9, 10] combined with the experimental data. The above range is found to fail to cover infra-red radiation adequately and needs to be extended to $1.5 \leqslant n \leqslant 4.0$ and $0.5 \leqslant k \leqslant 3.0$ to incorporate the soot property variation up to about 20 μm. Accordingly, the primary objective of the study is to produce the error contours representing the percent deviation involved with the Rayleigh limit and the Penndorf expansion relative to the Lorenz–Mie theory for the range $1.5 \leqslant n \leqslant 4.0$ and $0.5 \leqslant k \leqslant 3.0$ as a continuous function of n and k, thus providing a complete coverage for property range of particulate thermal radiation. The contours exhibit a distinguished error dependency on n with the dependency on k being of secondary importance. It is shown that for optical properties associated with infra-red radiation, Rayleigh deviation may well exceed 40% for $\alpha = 0.3$ while that of Penndorf remains within 5%. Likewise, for $\alpha = 0.7$, Rayleigh deviation reaches about 60% while that of Penndorf remains about within 10%. Thus, a basis is provided here for judging the accuracy of Rayleigh limit and Penndorf extension in the continuous n–k domain for the particulate radiation. The next section utilizes dispersion theory in computing n and k against wavelength and generates the extinction error contours for both Rayleigh and Penndorf approximations as a continuous function of m and discrete function of α. The study is concluded with some final remarks.

2. SMALL SIZE PARAMETER LIMIT OF LORENZ–MIE THEORY: ERROR CONTOURS EXTENDED VIA DISPERSION THEORY

The dependence of the soot optical properties—refractive index n and absorptive index k—on the wavelength has been studied by several researchers [9–14]. In terms of the Lorentz dispersion theory, Dalzell and Sarofim [9], and Lee and Tien [10] predicted

Table 1. Dispersion parameters from refs. [9, 10, 14]

Dispersion parameters	ref. [9]	ref. [10]	ref. [14]
$n_1 \times 10^{-27}\ \mathrm{m}^{-3}$	2.69	4.07	1.67
$n_2 \times 10^{-28}\ \mathrm{m}^{-3}$	2.86	4.47	1.83
$n_c \times 10^{-25}\ \mathrm{m}^{-3}$	406	4.0	0.7
$g_1 \times 10^{-15}\ \mathrm{s}^{-1}$	6	5.9	7
$g_2 \times 10^{-15}\ \mathrm{s}^{-1}$	7.25	5.6	7.25
$g_c \times 10^{-15}\ \mathrm{s}^{-1}$	6	1.2	1.2
$\omega_{01} \times 10^{-15}\ \mathrm{s}^{-1}$	1.25	1.25	1.25
$\omega_{02} \times 10^{-15}\ \mathrm{s}^{-1}$	7.25	7.25	7.25

$$m^2 = \left[1 + \frac{e^2}{m^*\varepsilon_0}\sum_j \frac{n_j(\omega_{0j}^2-\omega^2)}{(\omega_{0j}^2-\omega^2)^2+\omega^2 g_j^2} - \frac{e^2}{m^*\varepsilon_0}\frac{n_c}{(\omega^2+g_c^2)}\right] - i\left[\frac{e^2}{m^*\varepsilon_0}\sum_j \frac{n_j\omega g_j}{(\omega_{0j}^2-\omega^2)^2+\omega^2 g_j^2} + \frac{e^2}{m^*\varepsilon_0}\frac{n_c g_c}{\omega(\omega^2+g_c^2)}\right], \quad (1)$$

which yields n and k through

$$k = \frac{1}{\sqrt{2}}\{-\mathscr{R}(m^2) + \{[\mathscr{R}(m^2)]^2 + [\mathscr{I}(m^2)]^2\}^{1/2}\}^{1/2}, \quad (2)$$

$$n = -\mathscr{I}(m^2)/2k, \quad (3)$$

where symbols are given in the Nomenclature. Based on these two similar models,† the present study computes n and k as a function of wavelength in the range 0.4 μm $\leqslant \lambda \leqslant$ 20 μm for parameters given by refs [9, 10], and recently by [14] (see Table 1). The results are shown in Table 2 for selected wavelengths and depicted in Figs 1 and 2 with arrows on three curves indicating the direction of increasing wavelength. Also shown in Fig. 1 are the experimental data for m compiled from numerous sources including Figs 7 and 8 of Foster and Howarth [12], Table 3 (monodisperse analysis) of Charalampopoulos and Felske [13], Table 1 of Janzen [15], and Pluchino *et al.* [16]. The n–k pairs of ref. [12] were selected at λ = 2, 4, 6, 8, 10 μm. The data in Fig. 2 consist of soot from acetylene and propane diffusion flames of ref. [9] combined with that of premixed methane/oxygen flames of ref. [13] and a number of extreme n–k pairs taken from Fig. 1. Table 2 and Figs 1 and 2 suggest an optical range of $1.5 \leqslant n \leqslant 4.0$ and $0.5 \leqslant k \leqslant 3.0$ for sooty media, which now covers the variation of n and k in the near infra-red up to about λ = 20 μm, as well as in the visible range. For this established range, the study investigates next the error involved with the Rayleigh limit and the Penndorf expansion relative to the LM-theory as a continuous function of n and k. Note that, with the exception of a negligibly small number of data points, dispersion theory and the available

† The difference is in the treatment of conduction electron related mass.

NOMENCLATURE

D	diameter [m]
e	electron charge, 1.602189×10^{-19} C
g_c, g_j	damping constants for conduction and bound electrons [s^{-1}]
i	complex unit
$\mathscr{I}$	'the imaginary part of'
k	absorptive index
m	complex refractive index
m^*	electron mass, 9.109534×10^{-31} kg
n	refractive index
n_c, n_j	number densities of conduction and bound electrons [number of electrons m^{-3}]
M_j, N_j	functions of n and k, equations (6) and (8)
Q	efficiency factor
$\mathscr{R}$	'the real part of'.

Greek symbols

α	size parameter
ε_0	dielectric constant of vacuum, 8.854188×10^{-12} C^2 [N^{-1} m^{-2}]
λ	wavelength [m] or [μm]
ω	angular frequency [s^{-1}]
ω_{0j}	natural frequency of bound electrons [s^{-1}].

Subscripts

a	absorption
c	conduction electrons
e	extinction
j	bound electrons
s	scattering.

Superscripts

E	Exact (LM-theory)
P	Penndorf
R	Rayleigh.

data define a shaded area as shown in Fig. 2 for property variation of carbon and soot combined in the visible and near infra-red up to $\lambda = 20$ μm. The bounds of the shaded area are not intended to be absolute and are drawn somewhat approximately to represent the physically meaningful property range of carbon and soot particles.

The volumetric spectral coefficients of radiative transfer equation for a monodisperse medium with single and independent scattering are known to be directly proportional to efficiency factors, the geometric cross-section, and the number density of particles. In particular, the extinction efficiency factor which is the sum of absorption and scattering

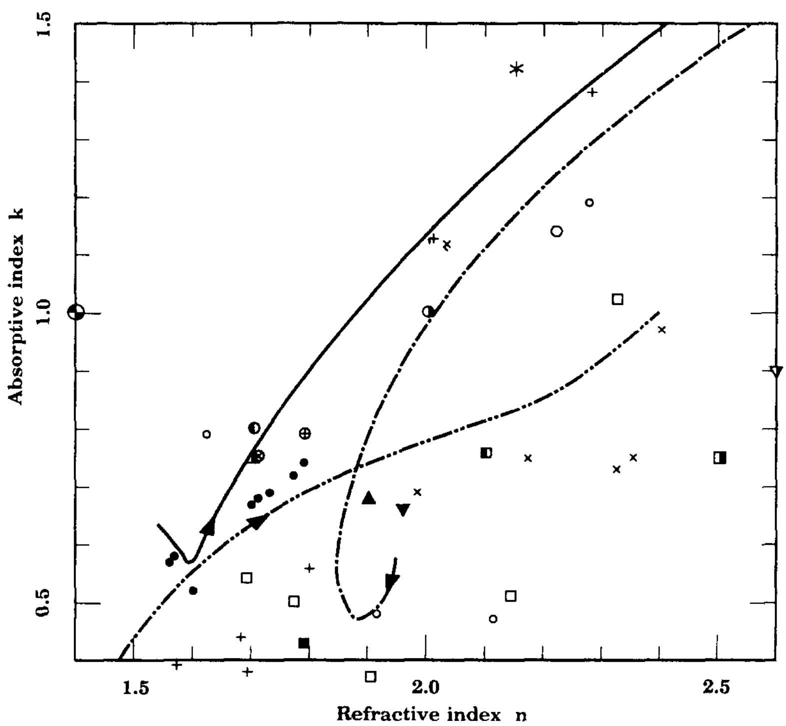

FIG. 1. Dispersion theory predictions and experimental results for optical properties of soot and carbon in the range $1.5 \leqslant n \leqslant 2.5$ and $0.5 \leqslant k \leqslant 1.5$. Dispersion parameters from: ——, Dalzell and Sarofim; —·—, Lee and Tien; —··—, Habib and Vervisch. Experimental data: ×, Sterling MT; ○, Vulcan 6; □, Elf 8; +, Mogul Plus [12]. ●, Charalampopoulos and Felske [13]. ẋ, Mukherjee; +, Huntjens and van Krevelen; *, McCartney and Ergun; ○, Ergun and McCartney; ■, Gilbert; ▼, Phillipp and Taft (graphite); Δ, Phillipp and Taft (vitreous carbon); ◧, Cosslett and Cosslett; ◨, DiNardo and Goland; ▲, Senftleben and Benedict ($\lambda = 0.436$ μm); ▼, Senftleben and Benedict ($\lambda = 0.546$ μm); ⊗, Stull and Plass ($\lambda = 0.436$ μm); ⊕, Stull and Plass ($\lambda = 0.546$ μm); ◍, Erickson *et al.* [15]. ◑, Janzen [15]. ◐, Pluchino *et al.* [16].

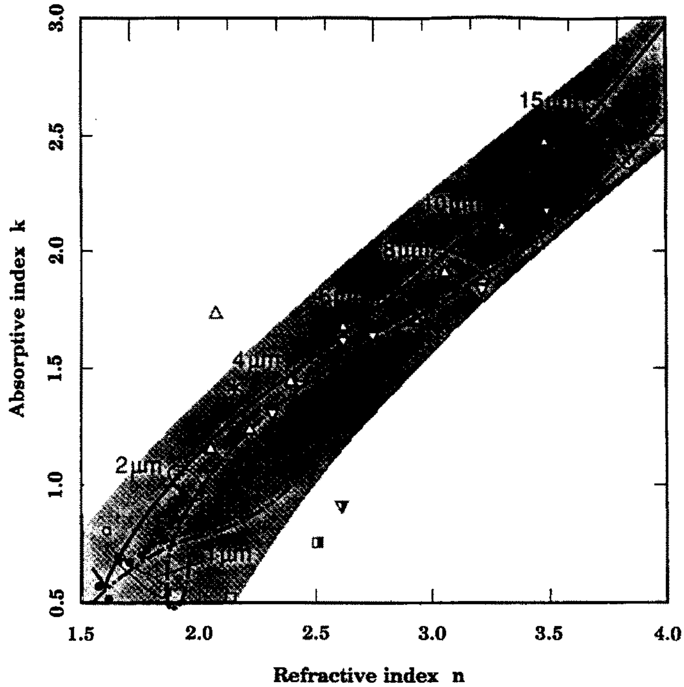

FIG. 2. Dispersion theory predictions and some experimental results for optical properties of soot and carbon in the range $1.5 \leqslant n \leqslant 4.0$ and $0.5 \leqslant k \leqslant 3.0$. ▽, Acetylene; △, Propane [9]. (The remaining legend is the same as Fig. 1.)

has been vastly used in the interpretation of optical diagnostics. Due to its significance and the additive feature, the extinction efficiency is chosen for the present investigation. The percent error for extinction is defined as

$$|\text{Error}|\% = \frac{|Q_e^{\text{R or P}} - Q_e^{\text{E}}|}{Q_e^{\text{E}}} \times 100, \quad (4)$$

where superscript E denotes the Exact (LM-theory) solution, R the Rayleigh limit, and P the Penndorf extension. While the details involving the computation of Q_e^E are described elsewhere [7], the expressions used for the Rayleigh limit and Penndorf extension are briefly described below.

In the well-known Rayleigh limit, the efficiency factors are

$$Q_e^R = Q_a^R + Q_s^R; \quad Q_a^R = 12(N_1/M_1)\alpha,$$
$$Q_s^R = \tfrac{8}{3}(1-3M_2/M_1)\alpha^4 \quad (5)$$

with subscripts a and s denoting absorption and scattering, respectively, and

$$M_1 = |2+m^2|^2 = N_1^2 + (2+N_2)^2, \quad M_2 = 1+2N_2,$$
$$N_1 = 2nk \equiv -\mathscr{I}(m^2), \quad N_2 = n^2 - k^2 \equiv \mathscr{R}(m^2), \quad (6)$$

where $m = n - ik$ is the usual complex refractive index of particles with respect to surrounding medium, i the complex unit and $\alpha = \pi D/\lambda$ is the size parameter, D the particle diameter, λ the wavelength; $\mathscr{R}$ indicates 'the real part of'; and $\mathscr{I}$,

Table 2. Soot refractive and absorptive indices from dispersion theory

	Dalzell and Sarofim [9]		Lee and Tien [10]		Habib and Vervisch [14]	
λ [μm]	n	k	n	k	n	k
0.4	1.538	0.640	1.952	0.678	1.381	0.388
0.5	1.577	0.577	1.932	0.532	1.415	0.314
0.6	1.591	0.567	1.902	0.482	1.423	0.278
0.7	1.603	0.582	1.879	0.474	1.424	0.262
1	1.653	0.682	1.847	0.546	1.426	0.264
2	1.906	1.037	1.987	0.963	1.474	0.395
4	2.399	1.486	2.517	1.476	1.676	0.617
6	2.769	1.759	2.929	1.721	1.869	0.727
8	3.047	1.972	3.222	1.887	2.015	0.784
10	3.267	2.164	3.439	2.032	2.122	0.820
15	3.699	2.614	3.830	2.393	2.289	0.901
20	4.057	3.036	4.137	2.757	2.392	0.997

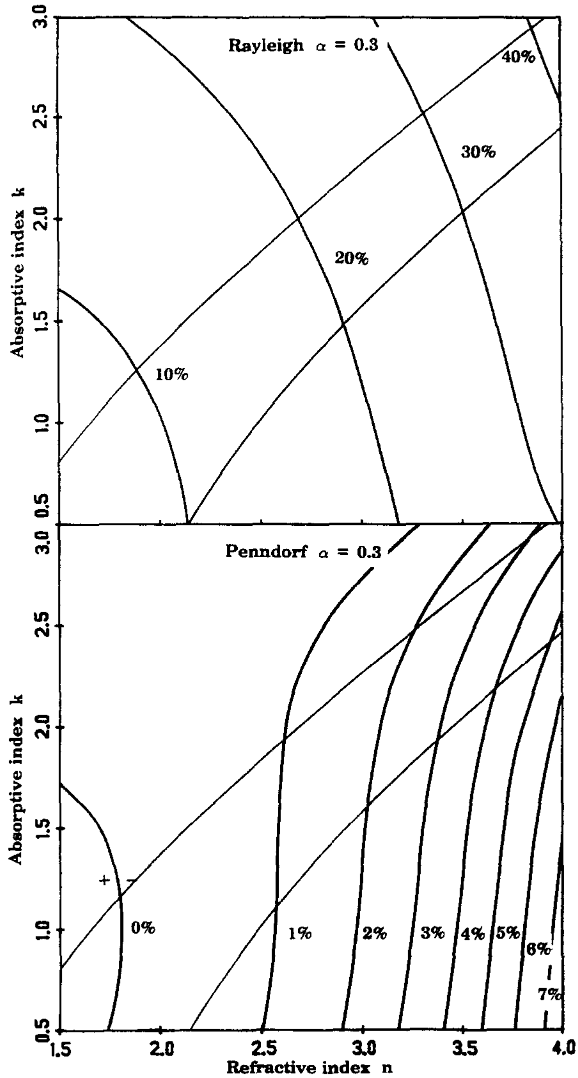

FIG. 3. The error contours for extinction efficiency in the Rayleigh limit and the Penndorf extension for $\alpha = 0.3$.

'the imaginary part of'. The foregoing results have been extended to larger particles by a series expansion [5]. For extinction efficiency factor, this expansion yields, after some rearrangement [7, 8],

$$Q_e^P = Q_a^R + 2\alpha^3\left[N_1\left(\frac{1}{15}+\frac{5}{3}\frac{1}{M_4}+\frac{6}{5}\frac{M_5}{M_1^2}\right)+\frac{4}{3}\frac{M_6}{M_1^2}\alpha\right], \quad (7)$$

with the remaining Ms and Ns defined as

$$M_4 = 4N_1^2+(3+2N_2)^2, \quad M_5 = 4(N_2-5)+7N_3,$$
$$M_6 = (N_2+N_3-2)^2-9N_1^2, \quad N_3 = (n^2+k^2)^2 = N_1^2+N_2^2. \quad (8)$$

The error contours generated in terms of equations (4)–(8) and the exact solution for the Rayleigh limit,† and the Penndorf extension are depicted in Figs 3, 4, and 5 for $\alpha = 0.3$, 0.5, and 0.7, respectively. The bounds of the shaded areas representing the soot index range discussed earlier illustrate nearly an order of magnitude better accuracy of Penndorf extension relative to the Rayleigh limit for smaller size parameter, and improved accuracy for larger size parameter. The inspection of Fig. 2 combined with Figs 3–5 also reveals that, for a given size parameter, the Rayleigh limit deteriorates sharply with increasing wavelength, thus with increasing n and k, whereas the Penndorf extension continues to remain close to the LM-theory.

Penndorf-based expressions become more significant for medium to large size soot particles. However, these particles are known, in most applications, to agglomerate to various shapes different than spheres, which may raise a question about the applicability of LM-theory. Yet, as Janzen [17] demonstrated, the volume equivalent spherical particle can characterize these nonspherical particles rather closely in certain applications. Chylek *et al.* [18] reached similar conclusions. Thus, in view of these works, LM-theory and its small size parameter approximations can be used for large soot particles. For recent studies on nonspherical particles, the reader is referred to refs [19–22].

† All error contours in Figs 3–5 for Rayleigh limit correspond to values lower than the LM-theory predictions.

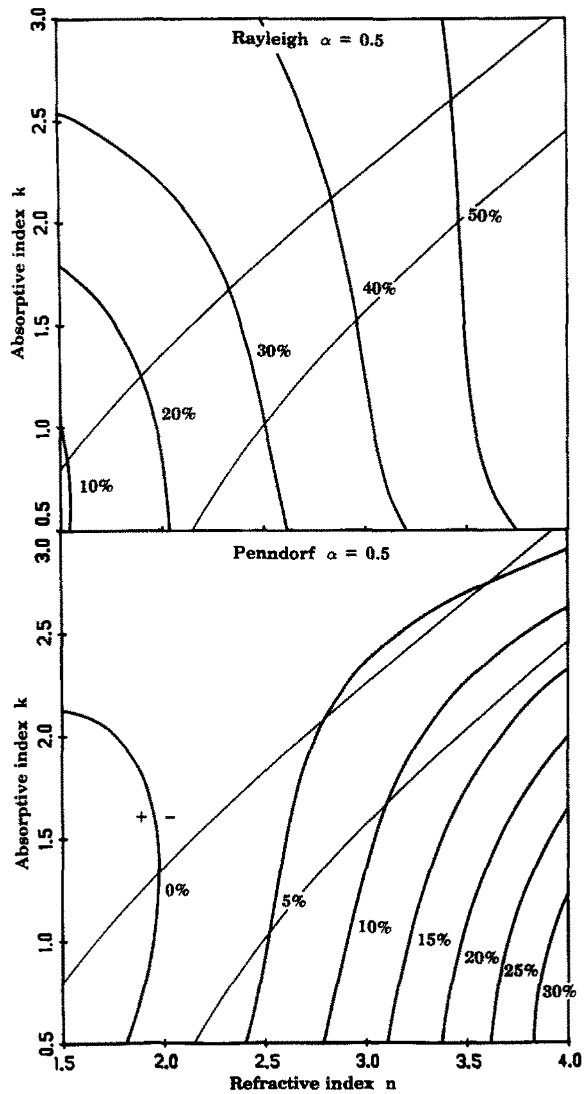

FIG. 4. The error contours for extinction efficiency in the Rayleigh limit and the Penndorf extension for $\alpha = 0.5$.

3. CONCLUDING REMARKS

The error contours representing the error committed by the Rayleigh limit and the Penndorf expansion relative to the LM-theory as continuous function of optical properties were extended to cover soot optical properties up to $\lambda \cong 20$ μm. In view of the Lorentz dispersion theory, this optical property range for soot was found to consist of $1.5 \leqslant n \leqslant 4.0$ and $0.5 \leqslant k \leqslant 3.0$. These contours facilitate an accurate assessment of the error resulting from the use of approximate expressions rather than the exact theory as a continuous function of optical properties and for a particular set of size parameters.

REFERENCES

1. C. L. Tien and S. C. Lee, Flame radiation, *Prog. Energy Combust. Sci.* **8,** 41–59 (1982).
2. R. Viskanta and M. P. Mengüç, Radiation heat transfer in combustion systems, *Prog. Energy Combust. Sci.* **13,** 97–160 (1987).
3. H. C. van de Hulst, *Light Scattering by Small Particles.* Wiley, New York (1957).
4. C. F. Bohren and D. R. Huffman, *Absorption and Scattering of Light by Small Particles.* Wiley, New York (1983).
5. R. B. Penndorf, Scattering and extinction coefficients for small spherical aerosols, *J. Atmos. Sci.* **19,** 193 (1962).
6. J. C. Ku and J. D. Felske, The range of validity of the Rayleigh limit for computing Mie scattering and extinction efficiencies, *J. Quant. Spectrosc. Rad. Tr.* **31,** 569–574 (1984).
7. A. Selamet, Radiation-affected laminar flame propagation, Ph.D. thesis, University of Michigan, Ann Arbor, Michigan (1989).
8. A. Selamet and V. S. Arpaci, Rayleigh limit—Penndorf extension, *Int. J. Heat Mass Transfer* **32,** 1809–1820 (1989).
9. W. H. Dalzell and A. F. Sarofim, Optical constants of soot and their application to heat flux calculations, *J. Heat Transfer* **91,** 100–104 (1969).
10. S. C. Lee and C. L. Tien, Optical constants of soot in hydrocarbon flames, Eighteenth Symposium (Inter-

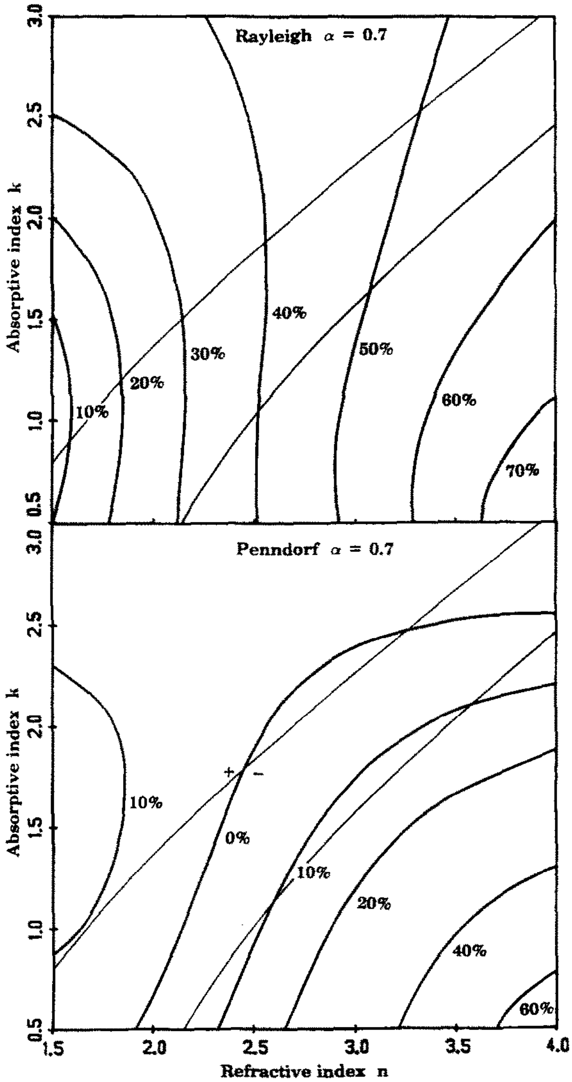

FIG. 5. The error contours for extinction efficiency in the Rayleigh limit and the Penndorf extension for $\alpha = 0.7$.

national) on Combustion, The Combustion Institute, Pittsburgh, pp. 1159–1166 (1981).

11. V. R. Stull and G. N. Plass, Emissivity of dispersed carbon particles, *J. Opt. Soc. Am.* **50,** 121–129 (1960).
12. P. J. Foster and C. R. Howarth, Optical constants of carbon and coals in the infra-red, *Carbon* **6,** 719–729 (1968).
13. T. T. Charalampopoulos and J. D. Felske, Refractive indices of soot particles deduced from *in-situ* laser light scattering measurements, *Combust. Flame* **68,** 283–294 (1987).
14. Z. G. Habib and P. Vervisch, On the refractive index of soot at flame temperature, *Combust. Sci. Technol.* **59,** 261–274 (1988).
15. J. Janzen, The refractive index of colloidal carbon, *J. Colloid Interface Sci.* **69,** 436–447 (1979).
16. B. Pluchino, S. S. Goldberg, J. M. Dowling and C. M. Randall, Refractive index measurements of single micron-sized carbon particles, *Appl. Optics* **19,** 3370–3372 (1980).
17. J. Janzen, Extinction of light by highly nonspherical strongly absorbing colloidal particles: spectrophotometric determination of volume distributions for carbon blacks, *Appl. Optics* **19,** 2977–2985 (1980).
18. P. Chylek, V. Ramaswamy, R. Cheng and R. G. Pinnick, Optical properties and mass concentration of carbonaceous smokes, *Appl. Optics* **20,** 2980–2985 (1981).
19. J. D. Felske, P.-F. Hsu and J. C. Ku, The effect of soot particle optical inhomogeneity and agglomeration on the analysis of light scattering measurements in flames, *J. Quant. Spectrosc. Rad. Transfer* **35,** 447–465 (1986).
20. B. L. Drolen and C. L. Tien, Absorption and scattering of agglomerated soot particulate, *J. Quant. Spectrosc. Rad. Transfer* **37,** 433–448 (1987).
21. D. W. Mackowski, R. A. Altenkirch and M. P. Mengüç, Extinction and absorption coefficients of cylindrically-shaped soot particles, *Combust. Sci. Technol.* **53,** 399–410 (1987).
22. D. W. Schuerman (Ed.), *Light Scattering by Irregularly Shaped Particles.* Plenum Press, New York (1980).